ESTIMATE OF THE SHIELDING EFFECTIVENESS OF AN ELECTRICALLY LARGE ENCLOSURE MADE WITH PIERCED METALLIC PLATE IN A WELL-STIRRED REVERBERATION CHAMBER

Angelo Gifuni*, Giuseppe Ferrara, Maurizio Migliaccio, and Antonio Sorrentino

Dipartimento di Ingegneria, Università Parthenope, Napoli 80143, Italy

Abstract—In this document, a simple and efficacious method to estimate the shielding effectiveness of an electrically large enclosure (SE_e) made with pierced metallic plate is shown under uniform and isotropic field conditions, which are produced in a reverberation chamber (RC) where the field is well stirred. The estimate is made by the calculation of the transmission cross sections (TCSs) of the walls of an enclosure and absorption cross sections (ACSs) of the inner losses. TCSs and ACSs are connected to the shielding effectiveness (SE) of the walls and inner losses, respectively; the latter are also connected to the reflectivity of the enclosure internal walls. The comparison with measurements made in an RC matches enough. It shows that the method shown here is sound. Moreover, the results support a recent model that connects SEe to SE by the reflectivity of the enclosure internal walls, and show still further that unloaded electrically large enclosures with distributed apertures are not very efficacious.

1. INTRODUCTION

Nowadays, with the growing development of wireless communications and diffusion of the electronic devices, it is more and more important to know the behavior of materials and enclosures, in terms of shielding effectiveness [1–12]. It is significant to estimate the shielding effectiveness of enclosures in a realistic electromagnetic environment, whose limit case is produced in a reverberation chamber (RC) when the field is well stirred [13–17].

The purpose of this document is to show a simple and efficacious method to estimate the shielding effectiveness of an electrically large enclosure (SEe) made with pierced metallic plate by the calculation of the transmission cross sections (TCSs) of its walls and absorption cross sections (ACSs) of the inner losses under uniform and isotropic field conditions. TCSs and ACSs are connected to the shielding effectiveness (SE) of the walls and inner losses, respectively; the latter are also connected to the reflectivity of the enclosure internal walls.

An RC is an electrically large cavity in which the field is properly randomized. In a well-stirred RC, the randomization is effective and the resulting field is uniform, isotropic and unpolarized. It is used to perform electromagnetic compatibility testing, including shielding effectiveness measurement of an enclosure [18]. However, an RC has a number of applications including antenna measurements, characterization of material properties, absorption of materials and biological bodies, and simulating various wireless multipath environments. An RC and an electrically large enclosure under test de facto form a nested reverberation chamber system [5, 7, 19]. It is important to note that the enclosure is uniformly and randomly fed from all sides; this tends to produce a field uniform and isotropic inside the enclosure as well. Clearly, the quality of the results depends on the real field conditions inside an enclosure. Strong loads shatter the assumed field conditions. If it is not otherwise specified, all relevant physical quantities are meant in the mean sense.

2. MODEL FOR SE_e OF AN ELECTRICAL LARGE ENCLOSURE

SEe can be defined as follows [7, 20]:

$$SE_{e(\text{dB})} = 10 \log \left(\frac{P_{rx,o}}{P_{rx,i}} \right) = 10 \log \left(\frac{\sigma_t + \sigma_{ae,i}}{\sigma_t} \right) \qquad (1)$$

where $P_{rx,o}$ is the power received by a receiving antenna placed in an RC and $P_{rx,i}$ the power received by a receiving antenna placed in the enclosure. Throughout the document, the subscript o (i) is referred to as the outer (inner) parameters; $\sigma_{ae,i} = \sigma_{w,i} + \sigma_{a,i} + A_e$ is the complete ACS inside the enclosure. $\sigma_{w,i}$ is the complete ACS of the enclosure walls when the field impinges from the inner of the enclosure; $\sigma_{a,i}$ is the ACS of the load; A_e is the effective area of the receiving antenna inside the enclosure. Finally, σ_t is the complete TCS of the walls of the enclosure under test. This last term includes the total leakage due to the enclosure wall junctions, possible apertures, feed points, and so on. In other words one sets $\sigma_t = \sigma_{tw} + \sigma_{tl}$, where σ_{tw} and σ_{tl} are the TCSs

of the walls and the one concerning the leakage, respectively. σ_{tw} and $\sigma_{w,i}$ are not independent.

For an enclosure without load ($\sigma_{a,i} = 0$), by neglecting A_e, (2) becomes:

$$SE_e = \frac{\sigma_t + \sigma_{w,i}}{\sigma_t}. \tag{2}$$

By considering an enclosure with negligible leakage ($\sigma_{tw} \gg \sigma_{tl} \Rightarrow \sigma_t \cong \sigma_{tw}$), (2) can be expressed as follows:

$$SE_e = SE\,(1 - R_{w,i}) \tag{3}$$

where SE is the shielding effectiveness of the walls and $R_{w,i}$ the reflectivity of the enclosure walls when the field impinges from the inner of the enclosure itself [21]. If $\sigma_{a,i}$ and σ_{tl} are not negligible, then one can write:

$$SE_e = SE_{eq}(1 - R_{eq,i}) \tag{4}$$

where SE_{eq} and $R_{eq,i}$ are an equivalent shielding effectiveness of the walls of an enclosure and the concerning equivalent reflectivity when the field impinges from the inner of the enclosure, respectively. For an unloaded enclosure ($\sigma_{a,i} = 0$) with negligible leakage, it turns out to be [21]:

$$SE \;=\; \sigma_{t,gA}/(\sigma_{tw}) \tag{5}$$
$$R_{eq,i} \;=\; \{\sigma_{a,gA} - [\sigma_{tw} + (\sigma_{w,i} + A_e)]\}/\sigma_{a,gA} \tag{6}$$

where $\sigma_{t,gA}$ is the TCS of the complete geometric area of the enclosure walls considered perfectly transmitting [20]. $\sigma_{t,gA}$ is quantitatively equal to $\sigma_{a,gA}$, which represents the ACS of the complete geometric area of the enclosure walls considered perfectly absorbing [20].

3. THE ABSORPTION COEFFICIENT OF A METALLIC SLAB

The absorption coefficient of an electrically large metallic slab of a given thickness placed in an electromagnetic environment, where the field is uniform and isotropic, can be achieved by the relative reflection coefficient. This can in turn be calculated from plane wave reflection coefficients at the interfaces for both the main polarizations. The two reflection coefficients are then squared, properly added and averaged over 2π sr, as shown below. This is equivalent to calculate $R_{w,i}$ from which is achieved the absorption coefficient. For completeness we show both the transmission and reflection coefficients. By transmission coefficients one could achieve SE; however, it is not proper for a pierced metallic slab. It is considered that the wave through the metallic slab

propagates orthogonally to the interface surface [22]. In actual fact, by considering Fig. 1, where s, ε and μ represent the conductivity, permittivity and permeability of the relative mediums, one can write:

$$\Gamma_v(\theta) = \rho_{v,12}(\theta) + \frac{\tau_{v,12}(\theta)\tau_{21}\rho_{21}e^{-j2k_2d}}{1 - (\rho_{21})^2 e^{-j2k_2d}} \tag{7}$$

$$\Gamma_h(\theta) = \rho_{h,12}(\theta) + \frac{\tau_{h,12}(\theta)\tau_{21}\rho_{21}e^{-j2k_2d}}{1 - (\rho_{21})^2 e^{-j2k_2d}} \tag{8}$$

$$T_v(\theta) = \frac{\tau_{v,12}(\theta)\tau_{21}e^{-jk_2d}}{1 - (\rho_{21})^2 e^{-jk_2d}} \tag{9}$$

$$T_h(\theta) = \frac{\tau_{h,12}(\theta)\tau_{21}e^{-jk_2d}}{1 - (\rho_{21})^2 e^{-jk_2d}} \tag{10}$$

where Γ_v and Γ_h represent the slab reflection coefficients for horizontal (perpendicular) and vertical (parallel) polarization, respectively. θ and d are the incidence angle and the thickness of the slab, respectively. ρ and τ are the reflection and transmission coefficients at the interfaces between the mediums, which are resolved by numeric subscript; the subscripts v and h mean that the polarization is vertical or horizontal, respectively. Also, the coefficients unmarked by subscript v and h refer at the normal incidence; clearly, they do not depend on θ.
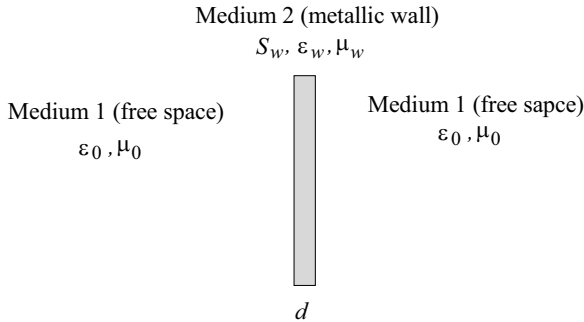

Figure 1. Electrically large metallic slab placed in an uniform and isotropic field.

For a plate with ordinary thickness one can write: $\Gamma_v(\theta) \cong \rho_{v,12}(\theta)$ and $\Gamma_h(\theta) \cong \rho_{h,12}(\theta)$; that is:

$$\alpha(\theta) = 1 - \frac{1}{2}\left(|\rho_{v,12}(\theta)|^2 + |\rho_{h,12}(\theta)|^2\right) \tag{11}$$

where $\alpha(\theta)$ is the absorption coefficient and $1/2$ equally accounts both

polarizations. In [23], it is shown that the term

$$\alpha = \int_0^{\pi/2} \alpha(\theta) \cos\theta \sin\theta d\theta, \tag{12}$$

which represents the average absorption coefficient of the solid part of pierced plate, can be expressed in the following analytical form:

$$\alpha = \frac{4}{3}\delta k_0 + \frac{1}{2}\left(\delta k_0\right)^2 \ln\left(\frac{\left(\delta k_0\right)^2}{2}\right) \cong \frac{4}{3}\delta k_0 = \frac{4}{3}\sqrt{\frac{4\pi\varepsilon_0 f}{s_w}} \tag{13}$$

where k_0 is the free-space wavenumber and f the frequency.

4. CALCULATIONS AND EXPERIMENTS

SE_e of a cubic $(0.5 \times 0.5 \times 0.5\,\mathrm{m}^3)$ enclosure made with pierced brass plate was calculated and measured. The conductivity of the solid part is $1.5E + 7\,\mathrm{S/m}$. The thickness of the walls is $0.5\,\mathrm{mm}$, the radius of the circular aperture is $1.5\,\mathrm{mm}$ and the distance between the near centres is $5\,\mathrm{mm}$. The ratio between open area and total geometric area is 32 per cent. The expected and measured SE_e can be easily achieved for such an enclosure; the leakage σ_{tl} can be neglected with respect to σ_t $(\sigma_{tw} \gg \sigma_{tl} \Rightarrow \sigma_t \cong \sigma_{tw})$. The leakage was however reduced to the minimum also by the use of adhesive aluminium tape on the unavoidable junctions. The walls of the enclosure are assumed locally planar; that is, the effect of the corners of the enclosure were neglected as well. The measurements were conducted in RC at the Università Parthenope; the RC used for the measurements is a cubic chamber of $8\,\mathrm{m}^3$ volume, where the input electromagnetic field is randomized by means of three metallic stirrers rotating in continuous mode. Random mechanical stirring due to the vibrations of the chamber walls under the effect of the motors of the stirrers adds up to the regular mechanical stirring so that a very large number of independent samples can be acquired. It must be noted that the statistically independence of the acquired samples was verified by the autocorrelation function (not shown to save space). The measurement set up include two double-ridge waveguide horn antenna and a two-ports Vectorial Network Analyzer (VNA), model Agilent 8363B PNA.

Figure 2 shows the experimental setup. A $30\,\mathrm{mm}$ monopole antenna is placed on one interior wall of the enclosure [7].

Figure 3 shows the enclosure inside the RC, and Fig. 4 shows a particular of the pierced brass plate.

By applying (1), in terms of power ratio, SE_e is achieved as follows [7]:

$$SE_{e(\mathrm{dB})} = \left\langle |S_{21}|^2 \right\rangle_{hh(\mathrm{dB})} - \left\langle |S_{21}|^2 \right\rangle_{hm(\mathrm{dB})} + \left(1 - |\langle S_{22}\rangle_{\mathrm{mm}}|^2\right)_{(\mathrm{dB})} \tag{14}$$
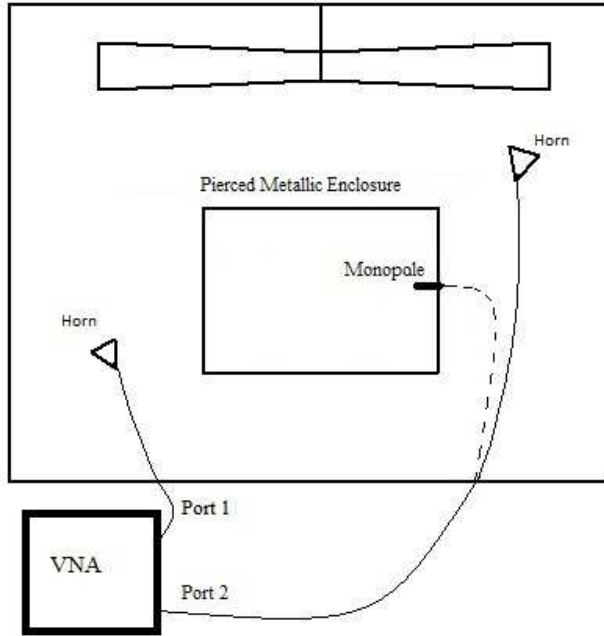
Figure 2. Experimental setup.

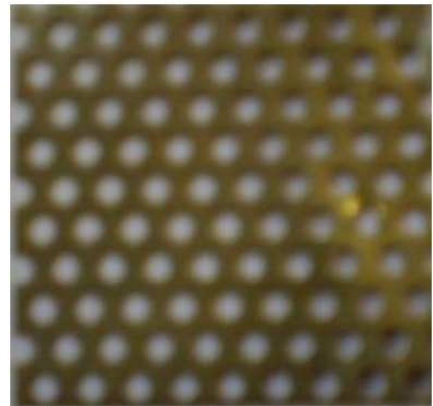**Figure 3.** Enclosure inside the RC.

Figure 4. Sample of the pierced brass plate forming the walls of the used enclosure.

where S_{21} and S_{22} represent the transmission and reflection coefficients (scattering parameters), respectively; the subscripts hh and hm denote the transmitting and receiving antennas, respectively; that is, hm means that the transmitting antenna is the horn whereas the one receiving is the monopole. The term in (14) including the coefficient S_{22} considers the impedance mismatch correction of the monopole. One notes that the impedance mismatch correction are absolutely marginal for the horn antennas in the used frequency range, so they are not included in (14). Two separate calibrations were performed, one for the transmission measurements and the other for the reflection measurements (continuous stirring). During the separate measurements of S_{21} and S_{22}, port 1 was stably connected to the transmitting horn antenna in RC; port 2 was instead consecutively connected to the receiving horn antenna in RC and to the monopole antenna on the interior wall of the enclosure, according to the setup shown in Fig. 2. These two successive transmission measurements are marked with hh (horn horn) and hm (horn monopole), respectively. The measurement set up was automatized with the software LabVIEV of National Instruments, so that, once the coefficient (S_{21} or S_{22}) was selected, 4000 independent samples were automatically acquired (for each frequency) in as many sweep frequency from 4 GHz to 18 GHz, with step of 0.2 GHz. The side 0.5 m of the cubic enclosure ranges from 6.67 to 30 lambda in the considered frequency range. For easiness, the field inside the enclosure was not further stirred as it was uniformly and randomly fed from all sides, and the enclosure was unloaded except for the effective area of the monopole; the ratio between the enclosure dimension and the minimum wavelength was greater than 6, and the SE_e was enough moderate at the set frequency range; all that supports the assumed field conditions inside the enclosure. Moreover, for that frequency range, the impedance mismatch of the monopole is generally low as well; however, its effect is shown in the results below.

The expected values of SE_e was achieved by means of the estimate of σ_t and $\sigma_{w,i}$ of the employed enclosure and by applying (4)–(6). σ_t was estimated for each hole as shown in [7, 20]. It is assumed that the holes are electromagnetically independent; $\sigma_{w,i}$ was estimated by means of the average absorption coefficient of the solid part of the enclosure walls.

One can write:

$$\sigma_{w,i} = \left(1 - R_{w,i} - \frac{1}{SE}\right)\sigma_{a,gA} = \alpha A_{g,sp} \qquad (15)$$

In short, by also considering (13), one can write [7, 20]:

$$\sigma_{w,i} = \left(\frac{4}{3} \sqrt{\frac{4\pi\varepsilon_0 f}{s_w}} 2C_1 \right) \sigma_{a,gA} \tag{16}$$

$$\sigma_t = \sum_1^N \frac{16}{9\pi} k_0^4 a^6 \tag{17}$$

where C_1 is a constant equal to the ratio between solid area and surface total area, a is the radius of the circular aperture, and N is the total number of circular aperture. For the used pierced plate $C_1 = A_{g,sp}/A_g = 0.68$, where $A_{g,sp}$ is the surface total area of the solid part of the walls, and A_g is the surface total area of the enclosure. One can also write [20, 21]: $A_g = 2\sigma_{a,gA} = 2\sigma_{t,gA}$. For convenience only, by also considering (5), Eq. (17) can be written as follows:

$$\sigma_t = \frac{16}{9\pi^2} k_0^4 a^4 \sum_1^N \pi a^2 = \left(\frac{16}{9\pi^2} k_0^4 a^4 2C_2 \right) \sigma_{t,gA} = \frac{\sigma_{t,gA}}{SE} \tag{18}$$

where C_2 is a constant equal to the ratio between open area and total geometric area, for the used pierced plate $C_2 = 0.32$.

By Considering that $\sigma_{t,gA}$ is quantitatively equal to $\sigma_{a,gA}$, and Eqs. (2), (16), and (18), one can write:

$$SE_e = \frac{\sigma_{w,i} + \sigma_t}{\sigma_t} = SE\,(1 - R_w)$$
$$= \frac{\left(\frac{8}{3} \sqrt{\frac{\pi\varepsilon_0 f}{s_w}} 2C_1 \right) \sigma_{a,gA} + \left(\frac{16}{9\pi^2} k_0^4 a^4 2C_2 \right) \sigma_{t,gA}}{\left(\frac{16}{9\pi^2} k_0^4 a^4 2C_2 \right) \sigma_{t,gA}}. \tag{19}$$

If one consider the dissipated power in the monopole load, then, by considering (4), (6) and ($\sigma_{t,l} = \sigma_{a,i} = 0$), one can write:

$$SE_e = SE\,(1 - R_w) + \frac{\frac{\left(1 - |\langle S_{22}\rangle|^2\right)c^2}{4\pi f^2}}{\left(\frac{16}{9\pi^2} k_0^4 a^4 2C_2 \right) \sigma_{t,gA}} = SE\,(1 - R_{eq}) \tag{20}$$

where c is the light speed, and the term $(1 - |\langle S_{22}\rangle|^2)$ again considers the impedance mismatch correction.

Figure 5 shows the experimental and expected SE_e; the latter is shown with and without the monopole load; when the monopole load is considered, the concerning impedance mismatch correction is considered as well. The measurement uncertainties are essentially the same as in [24]; that is, the standard uncertainty is generally less than 1 dB. Fig. 6 shows the ratio between A_e and $\sigma_{w,i}$, where the former is corrected for the impedance mismatch of the monopole.
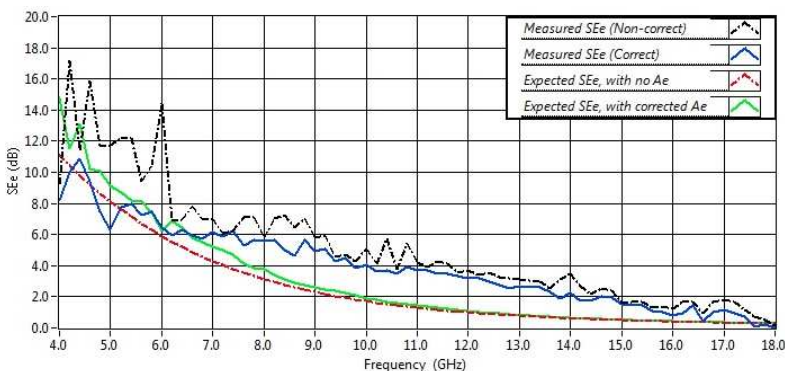
Figure 5. SE_e of an enclosure made with pierced brass plate, measured and theoretical. Theoretical curves are with no A_e (Eq. (19)) and with corrected A_e (Eq. (20)).
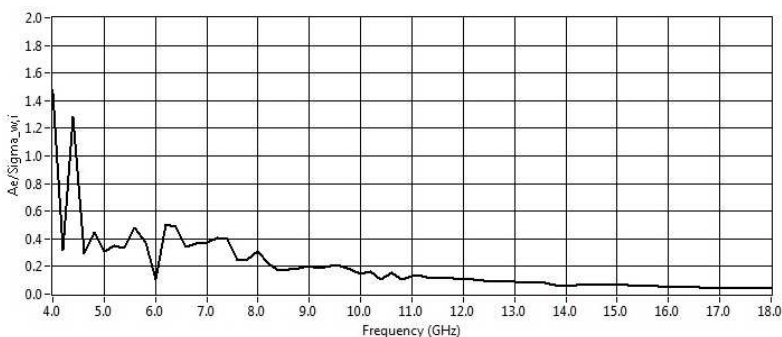

Figure 6. Ratio between A_e and $\sigma_{w,i}$; the former is corrected for impedance mismatch monopole.

One notes that the experimental and theoretical results match well enough. The differences between the expected values of SE_e and the measured ones are in part due to the measurement uncertainties. Hence, the simple method shown here to estimate the shielding effectiveness of an electrically large enclosure made with pierced metallic plate is sound. The results also support a recent model that connects SE_e to SE by the reflectivity of the enclosure internal walls, and show still further that unloaded electrically large enclosures with distributed apertures are not very efficacious.

We specify that the conditions $\sigma_{a,i} = 0$ determine the minimum value of SEe (worst case). The electronic devices, which are shielded by the enclosure, could load it in a way not negligible. However, we conservatively have shown the worst case of SE_e for the enclosure.

5. CONCLUSION

In this document, the shielding effectiveness of an electrically large enclosure made with pierced metallic plate was calculated and measured under uniform and isotropic field conditions. The calculation regards TCSs of the walls and ACSs of inner losses or equivalently the SE of the walls and the reflectivity of the enclosure internal walls. The measurements were made in a well-stirred reverberation chamber. Experimental and expected results match enough. This show that the estimation method for an electrically large enclosure made with pierced metallic plate is sound. The results also support a recent model that connects SE_e to SE by the reflectivity of the enclosure internal walls, and shows again that unloaded electrically large enclosures with distributed apertures are not very efficacious.

ACKNOWLEDGMENT

REFERENCES

1. Raj, C. D., G. S. Rao, P. V. Y. Jayasree, B. Srinu, and P. Lakshman, "Estimation of reflectivity and shielding effectiveness of three layered laminate electromagnetic shield at X-band," *Progress In Electromagnetics Research B*, Vol. 20, 205–223, 2010.

2. Bahadorzadeh Ghandehari, M., M. Naser-Moghaddasi, and A. R. Attari, "Improving the shielding effectiveness of a rectangular metallic enclosure with aperture by using extra shielding wall," *Progress In Electromagnetics Research Letters*, Vol. 1, 45–50, 2008.

3. Dehkhoda, P., A. Tavakoli, and R. Moini, "Fast calculation of the shielding effectiveness for a rectangular enclosure of finite wall thickness and with numerous small apertures," *Progress In Electromagnetics Research*, Vol. 86, 341–355, 2008.

4. Morari, C., I. Balan, J. Pintea, E. Chitanu, and I. Iordache, "Electrical conductivity and electromagnetic shielding effectiveness of siliconeb rubber filled with ferrite and graphite powders," *Progress In Electromagnetics Research M*, Vol. 21, 93–104, 2011.

5. Holloway, C. L., D. A. Hill, J. Ladbury, G. Koepke, and R. Garzia, "Shielding effectiveness measurements of materials using nested reverberation chambers," *IEEE Trans. on Electromagn. Compat.*, Vol. 45, 350–356, May 2003.

6. Gifuni, A. and M. Migliaccio, "Use of nested reverberating chambers to measure shielding effectiveness of nonreciprocal samples taking into account multiple interactions," *IEEE Trans. on Electromagn. Compat.*, Vol. 50, 783–786, Nov. 2008.

7. Holloway, C. L., D. A. Hill, M. Sandroni, J. Ladbury, J. Coder, G. Koepke, A. C. Marvin, and Y. He, "Use of reverberation chambers to determine the shielding effectiveness of physically small, electrically large enclosures and cavities," *IEEE Trans. on Electromagn. Compat.*, Vol. 50, 770–782, Nov. 2008.

8. Fang, C.-H., S. Zheng, H. Tan, D. Xie, and Q. Zhang, "Shielding effectiveness measurements on enclosures with various apertures by both mode-tuned reverberation chamber and GTEM cell methodologies," *Progress In Electromagnetics Research B*, Vol. 2, 103–114, 2008.

9. Mariani, P. V., F. Moglie, and A. P. Pastore, "Field penetration through a wire mesh screen excited by a reverberation chamber field: FDTD analysis and experiments," *IEEE Trans. on Electromagn. Compat.*, Vol. 51, No. 4, 883–891, Nov. 2009.

10. Lampasi, D. A. and M. S. Sarto, "Shielding effectiveness of a thick multilayered panel in a reverberating chamber," *IEEE Trans. on Electromagn. Compat.*, Vol. 53, No. 3, 579–588, Aug. 2011.

11. Van De Beek, S., R. Vogt-Ardatjew, H. Schipper, and F. Leferink, "Vibrating intrinsic reverberation chambers for shielding effectiveness measurements," *2012 International Symposium on Electromagnetic Compatibility (EMC EUROPE)*, 1–6, Rome, IT, Sep. 17–21, 2012.

12. Migliaccio, M., G. Ferrara, A. Gifuni, A. Sorrentino, F. Colangelo, C. Ferone, R. Cioffi, and F. Messina, "Shielding effectiveness tests of low-cost civil engineering materials in a reverberating chamber," *Progress In Electromagnetics Research B*, Vol. 54, 227–243, 2013.

13. Corona, P., G. Latmiral, E. Paolini, and L. Piccioli, "Use of reverberating enclosure for measurements of radiated power in the microwave range," *IEEE Trans. on Electromagn. Compat.*, Vol. 18, 54–59, May 1976.

14. Corona, P. and G. Latmiral, "Approccio termodinamico allo studio di una camera riverberante elettromagnetica a geometria variabile," Estratto dal Volume Studi in Onore di Giuseppe Simeon, Istituto Universitario Navale, 309–319, Napoli, Italy,

1978.

15. Corona, P., G. Latmiral, and E. Paolini, "Performance and analysis of a reverberating enclosure with variable geometry," *IEEE Trans. on Electromagn. Compat.*, Vol. 22, 2–5, Feb. 1980.

16. Hill, D. A., "Plane wave integral representation for fields in reverberation chamber," *IEEE Trans. on Electromagn. Compat.*, Vol. 40, No. 3, 209–217, Aug. 1998.

17. Gifuni, A., "On the expression of the average power received by an antenna in a reverberating chamber," *IEEE Trans. on Electromagn. Compat.*, Vol. 50, 1021–1022, Nov. 2008.

18. IEC 61000-4-21, "Electromagnetic compatibility (EMC), Part 4–21: Testing and measurement techniques — Reverberation chamber test methods," International Electrotechnical Commission, Geneva, Switzerland, 2003.

19. Hatfield, M. O., "Shielding effectiveness measurements of materials using mode-stirred chambers: A comparison of two approaches," *IEEE Trans. on Electromagn. Compat.*, Vol. 30, 229–238, Aug. 1988.

20. Hill, D. A., M. T. Ma, A. R. Ondrejka, B. F. Riddle, M. L. Crawford, and R. T. Johnk, "Aperture excitation of electrically large, lossy cavities," *IEEE Trans. on Electromagn. Compat.*, Vol. 36, 169–177, Aug. 1994.

21. Gifuni, A., "On the measurement of the absorption cross section and material reflectivity in a reverberation chamber," *IEEE Trans. on Electromagn. Compat.*, Vol. 51, 1047–1050, Nov. 2009.

22. Stratton, J. A., *Electromagnetic Theory*, McGraw-Hill, New York, 1941.

23. Gifuni, A., "Calcolo delle perdite elettromagnetiche nelle pareti delle camere riverberanti," *Annali Della Facoltà di Scienze e Tecnologie*, Università Degli Studi di Napoli "Parthenope", Napoli, 2004, ISSN 1825–1331.

24. Gifuni, A., A. Sorrentino, A. Fanti, G. Ferrara, M. Migliaccio, G. Mazzarella, and F. Corona, "On the evaluation of the shielding effectiveness of an electrically large enclosure," *Advanced Electromagnetics*, Vol. 1, No. 1, 84–91, May 2012.